OPTIMUM CONTROL OF THERMOELASTIC DEFORMATION IN A SMART COMPOSITE DISK

Fumihiro Ashida*, Theodore R. Tauchert**

* Department of Electronic Control and Systems Engineering, Shimane University, Shimane 690-8504, Japan ** Department of Mechanical Engineering, University of Kentucky, KY 40506-0503, USA

Summary This paper deals with a smart composite disk consisting of a structural layer onto which two piezoceramic layers are bonded. An unknown heating temperature distribution acting on the bottom surface is inferred from an electric potential distribution induced in the middle piezoceramic layer. A step-wise electric potential distribution applied to the top piezoceramic layer that controls a thermoelastic displacement distribution on the bottom surface is determined by optimization subject to stress constraints.

INTRODUCTION

By utilizing the direct and converse piezoelectric effects inherent in piezoelectric materials, functions called "selfmonitoring" and "self-control", which are essential for smart structures, can be achieved. For smart structures operating in thermal environments, materials must have heat resistance, high strength and high stiffness.

This paper deals with a smart composite circular disk that controls a thermoelastic deformation resulting from an unknown thermal load. The disk consists of a transversely isotropic structural layer and two piezoceramic layers of crystal class 6mm, as shown in Fig. 1. The middle piezoceramic layer serves as a sensor and the top piezoceramic layer serves as an actuator. An unknown heating temperature distribution acting on the bottom surface of the disk is inferred from the induced electric potential distribution assumed to be measured on the upper interface of the sensor layer. Then a step-wise electric potential distribution is applied to electrodes concentrically arranged on the top surface of the actuator layer in order to control the thermoelastic displacement distribution on the bottom surface of the disk. This problem is analyzed by means of the piezothermoelastic potential function approach [1]. The voltage applied to each electrode is determined by optimization using Fletcher-Reeves's conjugate gradient method, so that the difference between the induced and desired displacement distributions is minimized subject to stress constraints.

PROBLEM STATEMENT

Disk characteristics

The layers are numbered 1 to 3 from the bottom. The quantities in the i-th layer will be denoted by corresponding symbols with subscript i. The layer thicknesses are denoted by c_i . The top and bottom surfaces of the disk are taken to be traction-free, the layers are perfectly bonded at the interfaces, and the cylindrical edge of the disk is constrained against radial deformation and simply supported at the bottom. In this case the elastic boundary conditions are given by

$$\begin{split} &\sigma_{1zz} = \sigma_{1rz} = 0 \text{ on } z = 0, \quad \sigma_{3zz} = \sigma_{3rz} = 0 \text{ on } z = b_3 \\ &u_{ir} = u_{(i+1)r}, \quad u_{iz} = u_{(i+1)z}, \\ &\sigma_{izz} = \sigma_{(i+1)zz}, \quad \sigma_{irz} = \sigma_{(i+1)rz} \end{split} \right\} \text{ on } z = b_i \quad (i = 1, 2) \\ &u_{ir} = 0, \sigma_{irz} = 0 \text{ on } r = a \quad (i = 1 \sim 3), \quad u_{1z} = 0 \text{ at } r = a, z = 0. \quad (3) \end{split}$$

$$\sigma_{izz} = \sigma_{(i+1)zz}, \quad \sigma_{irz} = \sigma_{(i+1)rz}$$
 on $z = b_i$ $(i = 1,2)$ (2)

$$u_{ir} = 0$$
, $\sigma_{irz} = 0$ on $r = a$ $(i = 1 \sim 3)$, $u_{1z} = 0$ at $r = a$, $z = 0$. (3)

The lower interfaces of both piezoceramic layers are electrically grounded, while the upper interface of the sensor layer and the cylindrical edge of the disk are free of electric charge. Then the electric boundary conditions are given by

$$\Phi_i = 0 \text{ on } z = b_{i-1} \ (i = 2,3), \quad D_{2z} = 0 \text{ on } z = b_2$$
 (4)

$$D_{ir} = 0$$
 on $r = a$ $(i = 2,3)$ (5)

Electrodes Transversely isotropic structural laver Piezoceramic layers of crystal class 6mm

Fig. 1 Geometry of a smart composite disk.

where u_{ik} , σ_{ikl} , Φ_i and D_{ik} denote the elastic displacements, stresses, electric potentials and electric displacements.

Inverse problem

Both layer interfaces provide perfect thermal contact, heat convection occurs over the top surface of the disk, and the cylindrical edge is thermally insulated. In this case the thermal boundary conditions are

$$T_i = T_{i+1}, -\lambda_{iz} T_{i,z} = -\lambda_{(i+1)z} T_{(i+1),z} \text{ on } z = b_i \ (i=1,2), \quad T_{3,z} + h_t T_3 = 0 \text{ on } z = b_3$$
 (6)

$$T_i = T_{i+1}, -\lambda_{iz} T_{i,z} = -\lambda_{(i+1)z} T_{(i+1),z}$$
 on $z = b_i$ $(i = 1, 2), T_{3,z} + h_t T_3 = 0$ on $z = b_3$ (6) $T_{i,r} = 0$ on $r = a$ $(i = 1 \sim 3)$

where T_i are temperatures, λ_{ik} are coefficients of thermal conductivity and h_k is the boundary conductance.

For the composite disk under the above boundary conditions, it is assumed that an unknown heating temperature distribution $\Theta(r)$ acts on the bottom surface of the disk, the induced electric potential distribution is measured at some points on the upper interface of the sensor layer, the top surface of the disk is free of electric charge, and the measured electric potentials can be approximated by the function $V_0 v_m(r)$:

$$\Phi_2^T = V_0 v_m(r) \text{ on } z = b_2, \quad D_{3z}^T = 0 \text{ on } z = b_3$$
 (8)

where V_0 is a constant electric potential and superscript T designates quantities associated with the thermal loading. Instead of invoking the thermal boundary condition on the bottom surface of the disk, the electric boundary condition given in the first of Eqs. (8) is assumed to be available; thus this inverse problem is analyzed and temperatures, elastic displacements, electric potentials, stresses and electric displacements are obtained. The unknown heating temperature is deduced from the temperature in the structural layer by applying the thermal boundary condition on the bottom surface:

$$\Theta(r) = T_1 - T_{1,z} / h_b \text{ on } z = 0.$$
 (9)

Control problem

The control problem entails determination of the step-wise electric potential distribution that must be applied to the top surface of the disk,

$$\Phi_3^E = \sum_{k=1}^n V_k \left\{ H(r - r_k) - H(r - r_k - w) \right\} \text{ on } z = b_3$$
 (10)

so that the resultant axial elastic displacement on the bottom surface of the disk has a desired distribution $u_0 g(r)$:

$$u_{1z} = u_{1z}^T + u_{1z}^E = u_0 g(r) \text{ on } z = 0$$
 (11)

where H(r) is Heaviside's unit step function, u_0 is a constant elastic displacement, and superscript E designates quantities associated with the electric loading. The voltage V_k applied to each electrode is determined by optimization subject to stress constraints.

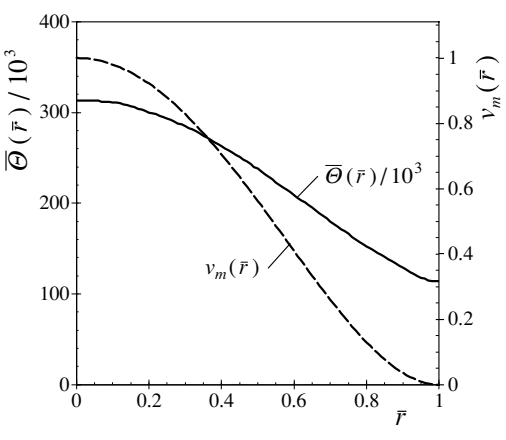


Fig. 2 Obtained heating temperature distribution.

NUMERICAL RESULTS

Numerical results are presented in terms of the following dimensionless quantities:

$$(\overline{r},\overline{z}) = \frac{(r,z)}{a}, \ (\overline{b}_{i},\overline{c}_{i},\overline{r}_{k},\overline{w}) = \frac{(b_{i},c_{i},r_{k},w)}{a}, \ B_{k} = a h_{k}, \ \overline{\Theta} = \frac{a \alpha_{1r} \Theta}{V_{0}|d_{21}|}, \ \overline{V}_{k} = \frac{V_{k}}{V_{0}}, \ \overline{u}_{ik} = \frac{u_{ik}}{V_{0}|d_{21}|}, \ \overline{\sigma}_{ikl} = \frac{a \sigma_{ikl}}{Y_{1r} V_{0}|d_{21}|}$$

where Y_{1r} is Young's modulus, α_{1r} is the coefficient of linear thermal expansion and d_{21} is the piezoelectric coefficient. Numerical calculations are carried out for a transversely isotropic graphite/epoxy composite layer and two cadmium selenide layers of crystal class 6mm [1]. The layer thicknesses and Biot's numbers are taken to be $\bar{c}_1 = 0.02$, $\bar{c}_2 = \bar{c}_3 = 0.001$, $B_b = 1$ and $B_t = 0.1$. The measured electric potentials are assumed to be approximated by the function $v_m(\bar{r}) = 1 - 2\bar{r}^2 + \bar{r}^4$. The desired elastic displacement distribution on the bottom surface of the disk is taken to be $g(\bar{r}) = 0$. The electrodes are arranged as $\bar{r}_k = 0.2(k-1)$ and $\bar{w} = 0.1$. For the stress constraints, the allowable

compressive, tensile and shear stresses of the cadmium selenide are assumed to be $(\overline{\sigma}_c^A, \overline{\sigma}_t^A, \overline{\sigma}_s^A) = (-150,10,10) \times 10^3$. To improve the convergence of response functions, the following function similar to the step function is used for the applied electric potential distribution:

$$\overline{\Phi}_{3}^{E} = \sum_{k=1}^{n} \overline{V}_{k} / [\{1 + e^{-250(\overline{r} - \overline{r}_{k})}\} \{1 + e^{250(\overline{r} - \overline{r}_{k} - \overline{w})}\}].$$

The distributions of measured electric potential and obtained heating temperature are illustrated in Fig. 2. Results for the applied voltages \overline{V}_k determined by optimization are shown in Table 1. In this table, n is the number of electrodes, $\overline{\sigma}_c$, $\overline{\sigma}_t$ and $\overline{\sigma}_s$ are the maximum values of the compressive, tensile and shear stresses induced in the cadmium selenide layers, f_{ob} is the value of the objective function defined by $f_{ob} = \sum_{j=0}^{100} [\overline{u}_{1z}(0.01j,0)/\overline{u}_{1z}^T(0.01j,0)]^2$, and R is the ratio of the maximum value of the controlled elastic displacement to that of

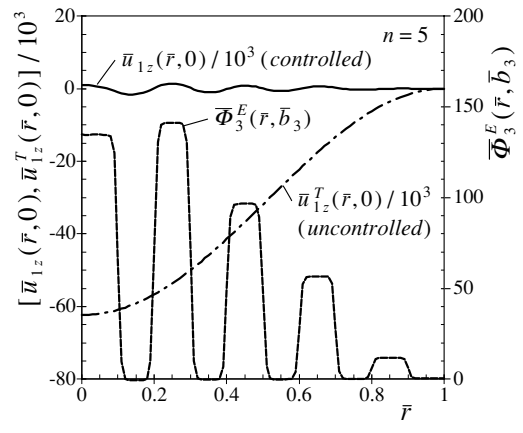


Fig. 3 Distribution of controlled elastic displacement.

uncontrolled elastic displacement on the bottom surface of the disk. It is seen that the maximum value of the controlled elastic displacement is reduced to about one fortieth of that of the uncontrolled elastic displacement in the case of n = 5 and the stress constraints are satisfied. For n = 5, the distributions of controlled and uncontrolled elastic displacements on the bottom surface as well as the applied electric potential distribution are illustrated in Fig. 3.

Table 1 Determined applied voltages, maximum stresses, and evaluations of optimization.

n	$\overline{V_1}$	\overline{V}_2	\overline{V}_3	\overline{V}_4	\overline{V}_5	$\overline{\sigma}_c/10^3$	$\overline{\sigma}_t/10^3$	$\overline{\sigma}_s/10^3$	f_{ob}	R [%]
1	129.81	_	_	_	_	-150.00	0.32	4.10	80.07	77.44
3	33.96	128.37	143.12	_	_	-150.00	0.82	4.58	2.18	11.98
5	135.36	141.69	96.92	56.66	11.50	-139.08	8.91	4.51	0.04	2.59

Reference

[1] Tauchert, T. R., Ashida, F.: Application of the Potential Function Method in Piezothermoelasticity: Solutions for Composite Circular Plates. *J. Thermal Stresses* **22**: 387-420, 1999.